

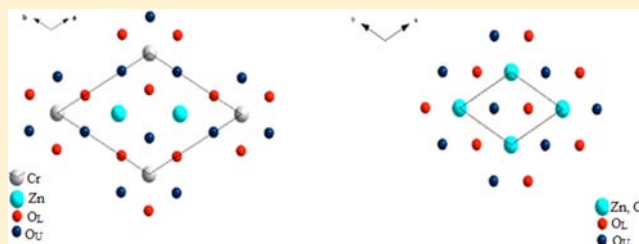
# Polytypism in Sulfate-Intercalated Layered Double Hydroxides of Zn and M(III) (M = Al, Cr): Observation of Cation Ordering in the Metal Hydroxide Layers

S. Radha and P. Vishnu Kamath\*

Department of Chemistry, Central College, Bangalore University, Bangalore-560 001, India

## S Supporting Information

**ABSTRACT:** The as-precipitated sulfate-intercalated layered double hydroxide of Zn and Al crystallizes in the structure of the  $3R_1$  polytype. On hydrothermal treatment, this  $3R_1$  polytype transforms into the somewhat rare  $3H$  and  $3R_2$  polytypes at different temperatures. Observation of the  $3R_2$  polytype distinct from the  $3R_1$  polytype is evidence for the lack of cation ordering in the  $[\text{Zn-Al-SO}_4]$  system. The layered double hydroxide of Zn and Cr (polytype,  $1H$ ) on hydrothermal treatment in mother liquor yields a cation-ordered phase also having the structure of the  $1H$  polytype. Direct evidence of cation ordering is found by the appearance of weak supercell reflections corresponding to  $a = \sqrt{3} \times a_0$  ( $a_0$  is the  $a$  parameter of the cation-disordered phase). The same precursor under other conditions yields the cation-disordered  $3R_1$  polytype. In this work, the structures of both the cation-ordered and the cation-disordered phases with similar states of hydration are refined and compared.



## INTRODUCTION

Most laboratory-synthesized layered double hydroxides (LDHs) crystallize with a plethora of structural disorders.<sup>1</sup> The disorder is of three varieties: (i) disorder in the stacking of the metal hydroxide sheets arising out of stacking faults and/or random intergrowth of more than one polytype, (ii) disorder in the interlayer, and (iii) intralayer disorder governing the position of the trivalent cation relative to the divalent cation. In the LDH literature, discussion of structural disorder is generally centered around the disorder in the stacking of the metal hydroxide layers.<sup>2–4</sup> This is because stacking disorders manifest themselves by the “anisotropic” broadening of peaks due to the different families of reflections in the PXRD pattern of the material.<sup>5</sup> The effect of intralayer cation disorder on the PXRD pattern is more subtle due to the poor intensity of the supercell reflections that arise out of cation order.<sup>6</sup> Consequently, there is comparatively less work on the nature and origin of cation order/disorder within the metal hydroxide layer. Investigation of these aspects requires samples with a very high degree of crystallinity. Single-crystalline samples of mineralogical origin have exhibited signs of cation ordering,<sup>7</sup> but in laboratory-synthesized samples the evidence is at best equivocal.

Synthesis under controlled conditions of pH and temperature sometimes yield products with better crystallinity.<sup>8</sup> Among the several methods known for laboratory preparation of LDHs, homogeneous precipitation under hydrothermal conditions and coprecipitation at constant pH are most effective in yielding ordered products.<sup>8–10</sup> In several instances, the as-synthesized LDH is subjected to hydrothermal treatment to improve the crystallinity of the product.<sup>11</sup> Hydrothermal treatment is known to bring about gel to crystallite conversions

among layered and microporous materials<sup>12</sup> and is also effective in eliminating stacking faults in certain materials. This is achieved either by treating the LDH powder in plain water or by treating the as-precipitated slurry in mother liquor at a high temperature in a closed reaction vessel. However, there are reports in the literature where hydrothermal treatment is known to facilitate only crystal growth without bringing about any structural order.<sup>13</sup> There are also reports where fast coprecipitation followed by hydrothermal treatment yields a stable suspension of LDH nanoplatelets whose size can be controlled by varying the temperature and duration of hydrothermal treatment.<sup>14</sup> Thus, hydrothermal treatment of LDHs is known to yield products with improved crystallinity as well as LDHs with altered structures.

Among LDHs intercalated with sulfate ions, the sulfate ion is known to intercalate with one of its  $C_3$  axes parallel to the stacking direction (also the  $c$ -crystallographic axis), reducing its symmetry from  $T_d$  to  $C_{3v}$ .<sup>15</sup> Sulfate-containing LDHs are known to crystallize with different levels of hydration wherein the water molecules are exchangeable.<sup>16</sup> They also are known to exist in several polytypic structures.<sup>17</sup> Hydrothermal treatment can potentially (i) bring about a change in the hydration levels of these materials, (ii) bring about interpolytype transitions, and (iii) alter the arrangement of water molecules and sulfate ions in the interlayer. Depending on the mechanism of the transformation under hydrothermal conditions several interesting results can thus be envisaged. While a mere rearrangement in the stacking of the metal

Received: October 21, 2012

Published: April 8, 2013

hydroxide layers could lead to improved crystallinity and/or polytype transformations, any dissolution and reprecipitation could potentially lead to a change in the cation arrangement in the layer and throw up interesting results.

In this paper we report hydrothermal treatment of sulfate-containing [Zn–Al] and [Zn–Cr] LDHs. Within the [Zn–Al] system we get some uncommon polytypes upon hydrothermal treatment. In the [Zn–Cr] system, we observe direct PXRD evidence for cation ordering within the metal hydroxide layers. We refine the structure by the Rietveld method and offer a structure model for a cation-ordered LDH.

## EXPERIMENTAL SECTION

**Synthesis.** [Zn–Al–SO<sub>4</sub>] and [Zn–Cr–SO<sub>4</sub>] LDHs were prepared by coprecipitation at constant pH and temperature (60 °C) as described elsewhere.<sup>18,19</sup> [Zn–Al–SO<sub>4</sub>] was precipitated in separate experiments at pH values of 8 and 9. [Zn–Cr–SO<sub>4</sub>] LDH was precipitated at pH 5.

**Hydrothermal Treatment.** After precipitation, a portion of the slurry was treated hydrothermally in mother liquor (HT) at 125 °C for a period of 24 h while the rest was aged at 60 °C for 18 h. The latter is here onward referred to as the as-prepared sample (ASP). Precipitates obtained in both cases were washed thoroughly with warm decarbonated water several times and finally with acetone. Products obtained were dried at room temperature and stored in airtight vials in a desiccator. As-prepared powder sample was also hydrothermally treated in plain water (HTPW) at 150 °C (24 h). Powder was then centrifuged, washed, and dried in a desiccator. The abbreviation used for each of these samples is listed in Table 1.

**Table 1. Total Water and Sulfate Contents Present in All Samples along with Approximate Formula**

LDH system	SO <sub>4</sub> <sup>2-</sup> content in mol ([Zn]:[Al]/[Cr]) <sup>a</sup>	water content (mol)	empirical formula
[Zn–Al]-8-ASP	0.149 (1.9)	0.84	[Zn <sub>0.654</sub> Al <sub>0.346</sub> (OH) <sub>2</sub> ](SO <sub>4</sub> ) <sub>0.15</sub> (CO <sub>3</sub> ) <sub>0.023</sub> ·0.84H <sub>2</sub> O
[Zn–Al]-8-HTPW-125	0.147 (1.8)	0.80	[Zn <sub>0.645</sub> Al <sub>0.355</sub> (OH) <sub>2</sub> ](SO <sub>4</sub> ) <sub>0.147</sub> (CO <sub>3</sub> ) <sub>0.03</sub> ·0.82H <sub>2</sub> O
[Zn–Al]-9-ASP	0.142 (2.1)	0.96	[Zn <sub>0.68</sub> Al <sub>0.32</sub> (OH) <sub>2</sub> ](SO <sub>4</sub> ) <sub>0.142</sub> (CO <sub>3</sub> ) <sub>0.018</sub> ·0.96H <sub>2</sub> O
[Zn–Al]-9-HTPW-125	0.144 (1.8)	0.81	[Zn <sub>0.645</sub> Al <sub>0.355</sub> (OH) <sub>2</sub> ](SO <sub>4</sub> ) <sub>0.144</sub> (CO <sub>3</sub> ) <sub>0.031</sub> ·0.81H <sub>2</sub> O
[Zn–Al]-9-HTPW-150	0.141 (1.9)	0.88	[Zn <sub>0.654</sub> Al <sub>0.346</sub> (OH) <sub>2</sub> ](SO <sub>4</sub> ) <sub>0.141</sub> (CO <sub>3</sub> ) <sub>0.032</sub> ·0.88H <sub>2</sub> O
[Zn–Cr]-ASP	0.148 (2.2)	0.77	[Zn <sub>0.685</sub> Cr <sub>0.315</sub> (OH) <sub>2</sub> ](SO <sub>4</sub> ) <sub>0.148</sub> (CO <sub>3</sub> ) <sub>0.009</sub> ·0.77H <sub>2</sub> O
[Zn–Cr]-HT-125	0.158 (2.2)	1.3	[Zn <sub>0.685</sub> Cr <sub>0.315</sub> (OH) <sub>2</sub> ](SO <sub>4</sub> ) <sub>0.158</sub> ·1.3H <sub>2</sub> O
[Zn–Cr]-HTPW-150	0.149 (2.3)	1.4	[Zn <sub>0.698</sub> Cr <sub>0.302</sub> (OH) <sub>2</sub> ](SO <sub>4</sub> ) <sub>0.149</sub> ·1.4H <sub>2</sub> O

<sup>a</sup>Values in parentheses are the [Zn]/[M<sup>3+</sup>] (M = Al, Cr) ratios as determined by AAS analysis.

**Characterization.** All samples were characterized by powder X-ray diffraction using a Bruker D8 Advance powder diffractometer (source Cu K $\alpha$  radiation,  $\lambda$  = 1.5418 Å). Data were collected at a scan rate of 1° 2 $\theta$  min<sup>-1</sup>. For structure refinement by the Rietveld method, data were collected at a step size of 0.02° 2 $\theta$  with a counting time of 6 s/step. IR spectra of the samples were recorded using Bruker model Alpha-P IR spectrometer (diamond ATR cell, 4 cm<sup>-1</sup> resolution, 400–4000 cm<sup>-1</sup>).

The metal content of all samples (Zn, Al, Cr) was determined by AAS-Optical Emission Spectroscopy (OES) a Varian model AA240 atomic absorption spectrometer. Na content of all samples was

estimated by flame photometry. [Zn]/[M] ratio was found to be in the neighborhood of 2 (Table 1) in all samples. The expected error in the AAS measurements is  $\pm 5\%$ . When the LDH solutions used for AAS-OES measurements were injected into a flame photometer, the Na content of all samples was below the detection level. To obtain a detectable level of Na, a large amount (0.06 g) of [Zn–Cr]-HT-125 sample was dissolved in a minimum amount of HCl and diluted to just 25 mL. This solution was injected without further dilution into the flame photometer. Measured Na content yielded a [Zn]/[Na] ratio  $\sim 298$ .

Sulfate content of the LDHs was determined by ion chromatography using a Metrohm model 861 Advanced Compact Ion Chromatograph fitted with a Metrosep SUP 5 150 column. For determining the anion content, a preweighed amount of the LDH was dissolved in a minimum amount of HCl and injected into the column. Standard solutions of sodium sulfate (Aldrich Chemical Co.) were used for calibrating the chromatograph response. Sulfate content in all samples was found to be lower than that required to compensate the positive charge predicted by the [Zn]/[M] (M = Al, Cr) ratio, indicating a slight carbonate contamination. For the purpose of this work, all samples reported here are treated as Na-free SO<sub>4</sub><sup>2-</sup>-LDHs.

Intercalated water content was determined by thermogravimetry using a Mettler Toledo TGA/SDTA 851<sup>+</sup>, star<sup>e</sup> 7.01 system (30–750 °C, heating rate of 5 °C min<sup>-1</sup>, flowing N<sub>2</sub>). Hydrated SO<sub>4</sub><sup>2-</sup>-LDHs are expected to have one intercalated water molecule per empirical formula unit. Observed water content was in the range 0.8–0.9 in most cases.

**Computational Studies.** All powder patterns were indexed using the PROZSKI suite of programs.<sup>20</sup> Lattice parameters were obtained using the program POWDER in conjunction with the lattice constant refinement program APPLEMAN and the figures of merit determined (Tables 2 and 3). Refinement of the structure of the 3R<sub>1</sub> polytype was

**Table 2. Observed and Calculated 2 $\theta$  Values of [Zn–Al–SO<sub>4</sub>] LDHs**

[Zn–Al]-8-HTPW-125 <i>a</i> = 3.13(1) Å <i>c</i> = 8.8 (5) Å FM (Mn) = 23.0		[Zn–Al]-9-ASP <i>a</i> = 3.066(6) Å <i>c</i> = 32.67(1) Å FM (Mn) = 12.5		[Zn–Al]-9-HTPW-125 <i>a</i> = 3.075(8) Å <i>c</i> = 26.43 (2) Å FM (Mn) = 19.0,		[Zn–Al]-9-HTPW-150 <i>a</i> = 3.072(1) Å <i>c</i> = 26.51 (3) Å FM (Mn) = 27.1	
2 $\theta$ (obs)	<i>hkl</i>	2 $\theta$ (obs)	<i>hkl</i>	2 $\theta$ (obs)	<i>hkl</i>	2 $\theta$ (obs)	<i>hkl</i>
10.1	001	8.16	003	10.08	003	10.08	003
20.1	002	16.23	006	20.15	006	20.2	006
33.7	100	24.52	009	30.3	009	30.5	009
35.2	101	33.89	101	33.77	101	33.8	101
39.5	102	34.23	012	35.18	103	36.35	104
45.9	103	36.54	015	36.4	104	41.5	107
60.2	110	40.54	018	39.35	106	48.45	1010
61.2	111	41.46	0015	41.5	107	56.65	1013
		45.85	0111	45.7	109	60.27	110
		60.41	110	48.5	1010	61.32	113
		61.0	113	60.2	110	64.3	116
		63.01	116	61.2	113		
				64.15	116		

carried out using the structure of the [Zn–Al–SO<sub>4</sub>] LDH (CC No. 91859) as the model. Coordinates corresponding to the metal hydroxide layer were used in the first phase of the refinement, and the coordinates of the anions were determined using the difference Fourier technique. The least-squares fitting technique as embodied in the GSAS program was used for structure refinement.<sup>21</sup>

No structure model is available for refinement of the cation-ordered 1H polytype of the [Zn–Cr–SO<sub>4</sub>] LDH. FOX (Free Objects for Crystallography), a structure optimization program, was used to obtain the initial structure.<sup>22,23</sup> FOX employs a reverse Monte Carlo approach, where starting from a random configuration the free

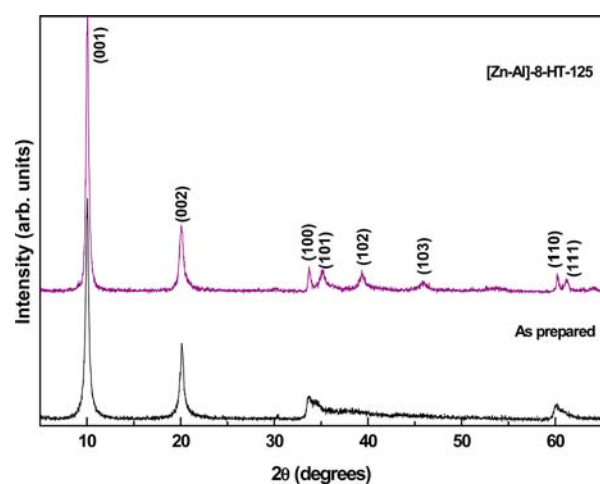
**Table 3.** Observed and Calculated  $2\theta$  Values of  $[\text{Zn-Cr-SO}_4]_{0.33}$  LDHs

as prepared $a = 3.119 \text{ \AA}$ $c = 8.93 \text{ \AA}$ FM (Mn) = 28.8		HT-125 $a = 5.414 \text{ \AA}$ $c = 11.065 \text{ \AA}$ FM (Mn) = 72.2		HTPW-150 $a = 3.118 \text{ \AA}$ $c = 32.552 \text{ \AA}$ FM (Mn) = 29.8	
$2\theta$ (obs)	$hkl$	$2\theta$ (obs)	$hkl$	$2\theta$ (obs)	$hkl$
9.9	001	8.0	001	8.1	003
19.9	002	16.0	001	16.3	006
30.0	003	18.9	100	24.6	009
33.3	100	20.5	101	33.2	101
34.7	101	24.1	003	35.3	104
38.9	102	33.1	110	36.0	015
45.3	103	34.1	111	40.0	018
53.2	104	37.0	112	45.4	0111
59.6	110	41.4	113	51.8	0114
60.4	111	47.0	114	59.2	110
		53.5	115	59.9	113
		59.1	300	61.9	116
		59.7	301		
		61.6	302		
		64.7	303		

parameters in the structure are varied randomly to minimize the cost function ( $R$  value). The only constraint used is antibump, which adds penalty when two atoms are closer than a minimum distance, specified by the user. Coordinates corresponding to the metal hydroxide layer were obtained by FOX. Using this partial structure, atomic coordinates corresponding to the interlayer atoms were then determined by the difference Fourier technique.

## RESULTS

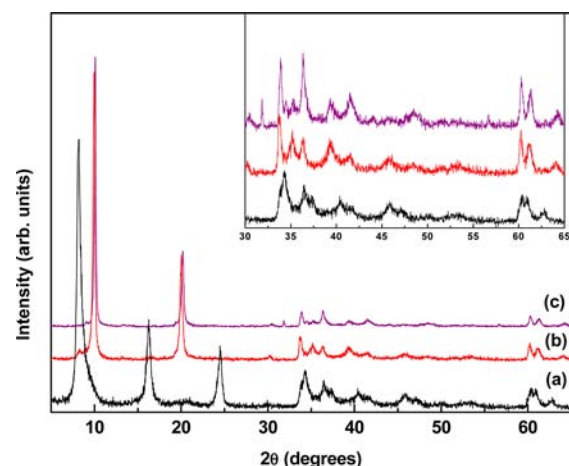
**$[\text{Zn-Al-SO}_4]$  LDH.** As-prepared  $[\text{Zn-Al}]$  LDH (pH 8) has a basal spacing of 8.8 Å and exhibits sawtooth-shaped reflections in the mid- $2\theta$  region indicative of turbostratic disorder (Figure 1). Upon hydrothermal treatment at 125 °C,

**Figure 1.** PXRD patterns of the  $[\text{Zn-Al}]$ -8-ASP LDH before and after hydrothermal treatment at 125 °C.

there is no change in the basal spacing. However, the PXRD pattern exhibits sharp reflections in the  $2\theta$  region 30–50°  $2\theta$  indicative of structural ordering. The pattern could be indexed to 1H polytype ( $a = 3.13 \text{ \AA}$ ,  $c = 8.8 \text{ \AA}$ , FOM = 23, Table 2).

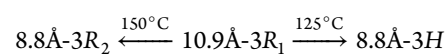
As-prepared  $[\text{Zn-Al}]$  LDH (pH 9) could be indexed to a 10.9 Å- $3R_1$  polytype. PXRD patterns corresponding to the

products of hydrothermal treatment of this sample at two different temperatures are shown in Figure 2. The LDH

**Figure 2.** PXRD patterns of the  $[\text{Zn-Al}]$  LDH (pH 9) (a) before and after hydrothermal treatment at (b) 125 and (c) 150 °C. (Inset) High-angle region in detail.

obtained at 125 °C has a lower basal spacing and is indexed to a three-layered unit cell with lattice parameters  $a = 3.075 \text{ \AA}$  and  $c = 26.43 \text{ \AA}$  (basal spacing 8.9 Å) (FOM = 19, Table 2). The presence of  $h0l$  reflections with  $l = 3n$  indicates that it belongs to hexagonal symmetry. As per Bookin and Drits,<sup>24</sup> there are seven different three-layer polytypes of hexagonal symmetry. From the data in Figure 2, it is difficult to precisely identify which of the seven hexagonal polytypes is obtained. The LDH obtained at 150 °C, on the other hand, could be indexed to a three-layered rhombohedral polytype ( $-h + k + l = 3n$ ). The appearance of strong  $h0l$  (104, 107, and 1010) reflections suggests crystallization of a  $3R_2$  polytype. This is a comparatively rare polytype with only one other report of its unequivocal synthesis.<sup>25</sup>

In conclusion, sample prepared at pH 9 upon hydrothermal treatment shows considerable changes in the stacking of the metal hydroxide slabs as well as in the extent of hydration. Observed transformations are summarized below



**$[\text{Zn-Cr-SO}_4]$  LDH.** The  $[\text{Zn-Cr}]$  LDH was prepared at pH 5. The PXRD patterns of the as-prepared and hydrothermally treated  $[\text{Zn-Cr}]$  LDHs are given in Supporting Information Figure S1. The as-prepared sample exhibits a high degree of order, and its structure has been refined to the 1H polytype.<sup>18</sup> Soon after precipitation, part of the slurry was hydrothermally treated at 125 °C in the mother liquor [HT-125] for a period of 18 h, and the corresponding PXRD pattern is shown in Figure 3 (also trace b in Supporting Information Figure S1). The  $[\text{Zn-Cr}]$ -HT exhibits a basal spacing of 11 Å corresponding to a bilayer arrangement of sulfate in the interlayer. The most striking feature is the presence of two weak reflections at  $2\theta$  values of 18.9° and 20.5°, which do not get indexed to any of the known phases with  $a = 2 \times d_{110}$ , corresponding to the cation-disordered structure model. The phase could however be indexed to a cation-ordered 1H polytype with a larger unit cell of  $a = 5.414 \text{ \AA}$  ( $a = \sqrt{3} \times a_0$ ). The two weak reflections are indexed as 100 and 101, respectively (Table 3). The  $[\text{Zn-Cr}]$  LDHs are known to

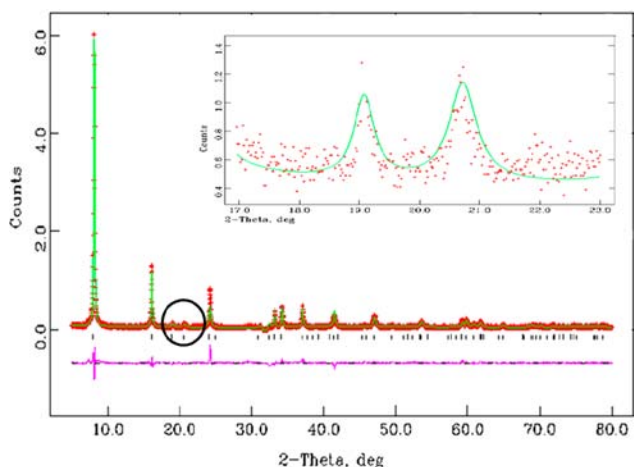


**Figure 3.** Rietveld fit of the PXRD pattern of the [Zn-Cr]-HT-125. (Inset) Details of the fit of the supercell reflections.

crystallize in the fixed composition  $[Zn]/[Cr] = 2$ ,<sup>26</sup> indicating the possibility of an ordered arrangement of cations in the layer. However, the supercell reflections, which provide direct evidence for cation ordering, are not reported. The intensity of any such reflections, if present, is computed to be  $\sim 0.1\%$  of the most intense peak.<sup>6</sup> The intensity of the observed supercell reflections in the present case is  $\sim 0.3\%$ . There are reports of cation-ordered structures among mineral forms of sulfate-LDHs.<sup>27,28</sup> Shigaita comprising of Al and Mn in the layer and nikischerite comprising Fe and Al in the layer are known to have cation-ordered structures. The structures of these minerals are solved by Hawthorne and co-workers using the  $R\bar{3}$  space group with a larger unit cell of  $a = 9.512 \text{ \AA}$  and  $c = 33.07 \text{ \AA}$ . While the authors claim the structure to be rhombohedral with a three-layered unit cell, reflection conditions do not meet the criterion  $-h + k + l = 3n$ . On the basis of the indexing we surmise that the crystal symmetry should be hexagonal. In the present case all observed reflections could be indexed to a one-layered hexagonal unit cell with  $a = 5.414 (4) \text{ \AA}$  and  $c = 11.06 (5) \text{ \AA}$  with an acceptable figure of merit (FOM = 72, Table 3). Thus, the model described by Hawthorne<sup>27,28</sup> cannot be used for structure refinement of the observed phase. On the basis of the reflection conditions, among the several possible space groups we chose  $P\bar{3}$  for structure solution as it provides appropriate special positions for the metal ions and the hydroxyl O atoms. We place the two metals Zn and Cr in  $2d$  and  $1a$  positions, respectively. Hydroxyl O was placed in a random position. Sulfate and water were added as molecules and placed in a random position in the interlayer. The code FOX was used to optimize the structure. Several snapshots taken during optimization are shown in Supporting Information Figure S2. The final optimized structure yielded a good model for the metal hydroxide layer as the intralayer metal–oxygen bond lengths and bond angles were in the range expected of the LDH layer. Positions of the intercalated sulfate molecules were rejected as they were found to be too close to the layer. The initial cycles of Rietveld refinement were carried out using the partial structure model obtained from FOX. The Fourier map of the difference profile was computed to get the residual electron density using the least-squares fitting program GSAS. A maximum in the residual electron density was found at the  $2c$  position  $(0, 0, 0.35)$ . The S atom was placed in this site and the occupancy refined. After further cycles of refinement, the

difference Fourier map was once again computed to determine the positions of the other interlayer atoms. The fit obtained after final refinement including all interlayer atoms is shown in Figure 3 (see Table 4 for the goodness of fit parameters). In

**Table 4.** Results of the Rietveld Refinement of [Zn-Cr]-HT-125 LDH

molecular formula	$[Zn_2Cr(OH)_6][SO_4]_{0.5} \cdot 4H_2O$
cryst syst	hexagonal
space group	$P\bar{3}$
cell params/ $\text{\AA}$	$a = 5.414 (2)$ ; $c = 11.07 (5)$
vol./ $\text{\AA}^3$	280.89
no. of data points	3713
no. of reflns fitted	176
$R_{wp}$	0.152
$R_p$	0.119
$R(F^2)$	0.121
$R_{exp}$	0.070
reduced $\chi^2$	2.38

particular, the computed pattern accounts for the weak reflections in the  $18\text{--}21^\circ$   $2\theta$  region which we ascribed to cation ordering. The position parameters, bond lengths, and bond angles are listed in Table 5. The structure obtained after

**Table 5.** Refined Atomic Position Parameters of the [Zn-Cr]-HT-125 LDH

atom	Wyckoff position	$x$	$y$	$z$	SOF
Zn	$2d$	0.6667	0.3333	0.000	0.33
Cr	$1a$	0.000	0.000	0.000	0.33
O1	$6g$	$-0.0029(9)$	$0.312 (2)$	$0.0782(1)$	0.33
S	$2c$	0.000	0.000	$0.35(4)$	0.08
O <sub>a</sub>	$2c$	0.000	0.000	$0.46 (2)$	0.08
O <sub>b</sub>	$6g$	0.000	$0.25(1)$	$0.3199(3)$	0.08
O <sub>w</sub>	$6g$	0.6000	0.3000	$0.714(8)$	0.19
		distances ( $\text{\AA}$ )		angles (deg)	
Zn–O1	$2.0631 (9)$	O1–Zn–O1	$103.617 (2)$		
Zn–O1	$2.0416 (9)$	O1–Zn–O1	$80.779 (1)$		
Cr–O1	$1.9071 (9)$	O1–Cr–O1	$100.97 (7)$		
S–O <sub>a</sub>	$1.229 (6)$	O1–Cr–O1	$79.023 (3)$		
S–O <sub>b</sub>	$1.393 (4)$	O <sub>a</sub> –S–O <sub>b</sub>	$103.840 (1)$		
S–O <sub>w</sub>	$2.901 (1)$	O <sub>b</sub> –S–O <sub>b</sub>	$114.460 (1)$		
O <sub>a</sub> –O <sub>w</sub>	$3.8152 (1)$				
O1–O <sub>a</sub>	$4.554 (1)$				
O1–O <sub>b</sub>	$2.712 (4)$				
O1–O <sub>w</sub>	$2.8021 (2)$				

final refinement is shown in Figure 4. Zn and Cr are present in two distinct sites and ordered along the  $a$  as well as the  $b$  axes. The Zn–O ( $2.01 \text{ \AA}$ ) bond distance is larger compared to that of Cr–O ( $1.9 \text{ \AA}$ ) as expected and the octahedra slightly distorted. The S atom of the sulfate ion occupies the  $2c$  position, while the O atoms occupy two different sites. One of the S–O bonds is parallel to the  $c$  axis, and this O is referred as apical atom O<sub>a</sub>. The apical O is in the  $2c$  site, whereas the other O<sub>b</sub> (basal O) atoms are in the  $6g$  site. The O–S–O bond angles ( $114^\circ$ ,  $103^\circ$ ) are different from that of the free sulfate ion ( $109^\circ$ ). This deviation is due to its interaction with the layer. This reduces the sulfate molecular symmetry from  $T_d$  (free ion) to  $C_{3v}$  (intercalated). Figure 4b shows the structure of the interlayer along with the lower and upper hydroxyl O of

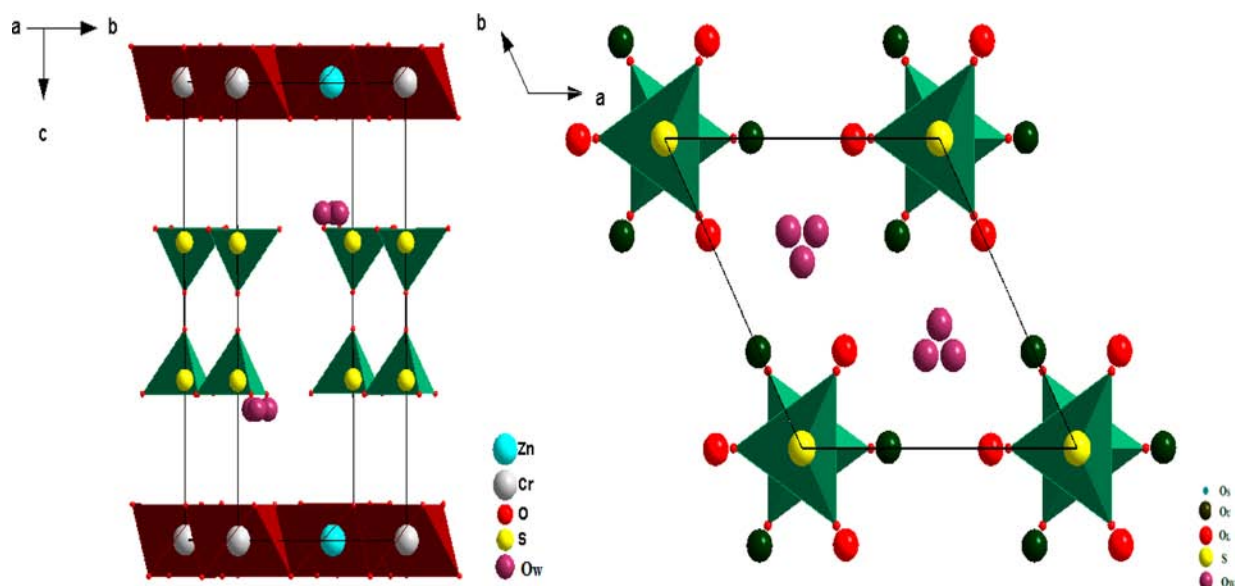


**Figure 4.** (a) Structure of the [Zn-Cr]-HT-125 LDH; (b) interlayer structure with the lower and upper hydroxyl O of adjacent layers.

the adjacent layers. The S atom of sulfate occupies the octahedral interlayer site. The  $O_b$  atoms of sulfate which are oriented toward the layer are in line with the hydroxyl O, thus promoting H bonding between the layer and the interlayer. The S- $O_b$  bond distances are slightly larger than the S- $O_a$  bond distance due to hydrogen bonding. The O atoms of water molecules occupy the  $6g$  sites and are disordered in the interlayer. Water O atoms are present in alternative octahedral sites which are distorted slightly due to distortion in the  $[Zn(OH)_6]$  octahedra. They are present at an H-bonding distance with the sulfate O as well as the hydroxyl O atoms. There is however no H bonding between the apical  $O_a$  of the  $SO_4^{2-}$  ion and the O atoms of the hydroxyl groups.

One of the characteristics of other cation-ordered hydroxide phases<sup>27–30</sup> is a sulfate content higher than that required by the need to compensate for the positive charge on the metal hydroxide layer. The excess sulfate is intercalated along with  $Na^+$  ions in the interlayer in the manner of ion pairs. The appearance of weak supercell reflections is thought to be related to the orderly arrangement of  $Na^+$  ions in the interlayer.<sup>30</sup> The Na content of mineral nikischerite is considerable at  $[M^{II}]/[Na] \approx 6$ .<sup>28</sup> The [HT-125] phase reported here does not have excess sulfate and only a negligible amount of Na at  $[Zn]/[Na] \approx 298$ . To further illustrate the effect of interlayer Na on the relative intensities of the supercell reflections, we compare in Supporting Information Figure S3 the simulated powder patterns (POWDERCELL) of [HT-125] with that of mineral nikischerite. We also simulate the powder pattern of [HT-125] by including in the interlayer (site 1b) a proportion of Na similar to that observed in nikischerite. It is seen that the supercell reflections are generated both in the presence and in the absence of interlayer Na. Further, in both Na-containing phases, the supercell reflection at  $18.9^\circ 2\theta$  diminishes in intensity when compared to the pattern of the Na-free phase. Thereby, the supercell reflections observed in the PXRD pattern of [HT-125] are due to the intrinsic intralayer ordering of cations.

The PXRD pattern of the LDH obtained by hydrothermally treating the as-synthesized sample at  $150^\circ C$  in plain water (HTP) (Figure 5 and trace c in Supporting Information Figure

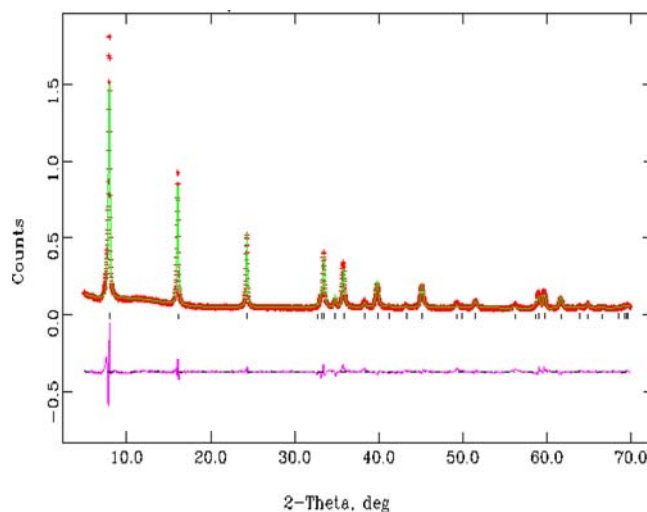


**Figure 5.** Rietveld fit of the PXRD pattern of the [Zn-Cr]-HTPW-150 LDH.

S1) exhibits a  $11 \text{ \AA}$  phase, which could be indexed to a three-layered rhombohedral polytype ( $a = 3.11 \text{ \AA}$ ,  $c = 32.55 \text{ \AA}$ ; FOM = 29). The presence of strong  $0kl$  reflections indicates that it is a  $3R_1$  polytype. A similar phase can also be obtained by mere hydration of the as-prepared sample. Our earlier attempt<sup>18,19</sup> to simulate this phase was unsuccessful due to the lack of a suitable structure model. Using the partial structure model of the reported  $25.4 \text{ \AA}$ - $3R_1$  phase (CC no. 91859), we arrive at the structure of the observed phase using the Rietveld method combined with the difference Fourier technique. Initially the coordinates corresponding to the single layer were used for refinement of the observed phase, and the  $z$  coordinate of the hydroxyl O was refined freely. Later the Fourier transform of the difference profile was computed as described earlier to determine all atomic positions in the interlayer. The fit obtained after including all interlayer atoms is shown in Figure 5, and the goodness of fit parameters are listed in Table 6. The plot of the structure obtained is shown in Figure 6. Both metal atoms occupy the same position as in other cation-disordered

**Table 6.** Results of the Rietveld Refinement of [Zn–Cr]-HTPW-150 LDH

molecular formula	[Zn <sub>2</sub> Cr(OH) <sub>6</sub> ][SO <sub>4</sub> ] <sub>0.5</sub> ·4H <sub>2</sub> O
cryst syst	rhombohedral
space group	<i>R</i> -3 <i>m</i>
cell params/Å	<i>a</i> = 3.125 (1); <i>c</i> = 32.835 (1)
vol./Å <sup>3</sup>	277.82
no. of data points	3822
no. of reflns fitted	73
<i>R</i> <sub>wp</sub>	0.113
<i>R</i> <sub>p</sub>	0.085
<i>R</i> ( <i>F</i> <sup>2</sup> )	0.146
<i>R</i> <sub>exp</sub>	0.055
reduced $\chi^2$	9.5

structures. The M–O bond distances and O–M–O bond angles are in the expected regime as in other LDHs and are reported in Table 7. Examination of the interlayer structure (Figure 6b) shows that the S atom of the sulfate and its apical O atom occupy 6*c* positions. The S atom is at the center of the prismatic interlayer site formed by the hydroxyl O atoms of adjacent layers. The basal O of the sulfate ion occupies the 18*h* site which are around the hydroxyl O of the layer and promote H bonding. The water O atoms occupy the other set of 18*h* sites and are at hydrogen-bonding distance with the layer and the sulfate. Comparison of the structure of a single layer corresponding to the ordered and disordered arrangement of the cations in the layer obtained by refinement of the two sulfate LDHs described above is shown in Figure 7. The cation-ordered structure has a larger *a* parameter corresponding to  $\sqrt{3} \times a_0$  and is similar to the one observed for [Li–Al] LDHs.<sup>31</sup>

**Table 7.** Refined Atomic Position Parameters of the [Zn–Cr]-HTPW-150 LDH

atom	Wyckoff position	<i>x</i>	<i>y</i>	<i>z</i>	SOF
Zn	3 <i>a</i>	0.000	0.000	0.000	0.67
Cr	3 <i>a</i>	0.000	0.000	0.000	0.331
O1	6 <i>c</i>	0.000	0.000	0.3571(3)	1.0
S	6 <i>c</i>	0.000	0.000	0.1434(1)	0.078
O <sub>a</sub>	6 <i>c</i>	0.000	0.000	0.1855(5)	0.078
O <sub>b</sub>	18 <i>h</i>	–0.583(9)	0.583(9)	0.205(1)	0.08
O <sub>w</sub>	18 <i>h</i>	0.8413(2)	0.8413(2)	0.0989(8)	0.2
distances (Å)		angles (deg)			
Zn(Cr)–O1	1.966 (69)	O1–Zn(Cr)–O1	105.265 (2)		
S–O <sub>a</sub>	1.382 (1)	O1–Zn(Cr)–O1	74.735 (1)		
S–O <sub>b</sub>	1.444 (4)	O <sub>a</sub> –S–O <sub>b</sub>	110.03 (2)		
S–O <sub>w</sub>	3.134 (1)	O <sub>b</sub> –S–O <sub>b</sub>	108.905 (3)		
O <sub>a</sub> –O <sub>w</sub>	2.850 (8)				
O1–O <sub>a</sub>	4.454 (2)				
O1–O <sub>b</sub>	3.264 (1)				
O1–O <sub>w</sub>	2.919 (6)				

While the cation-ordered layer belongs to the layer group *P*-312/*m*, the cation-disordered layer belongs to *P*-32/*m*1.

## DISCUSSION

The ordering of M<sup>II</sup> and M<sup>III</sup> in the LDH layer has been a subject of considerable debate in the LDH literature for the past several years.<sup>32–36</sup> Strong evidence for the local ordering of cations is provided by NMR and EXAFS studies which probe the short-range structure.<sup>32,33</sup> Both techniques have been employed to study several LDH systems including [Mg–Al],

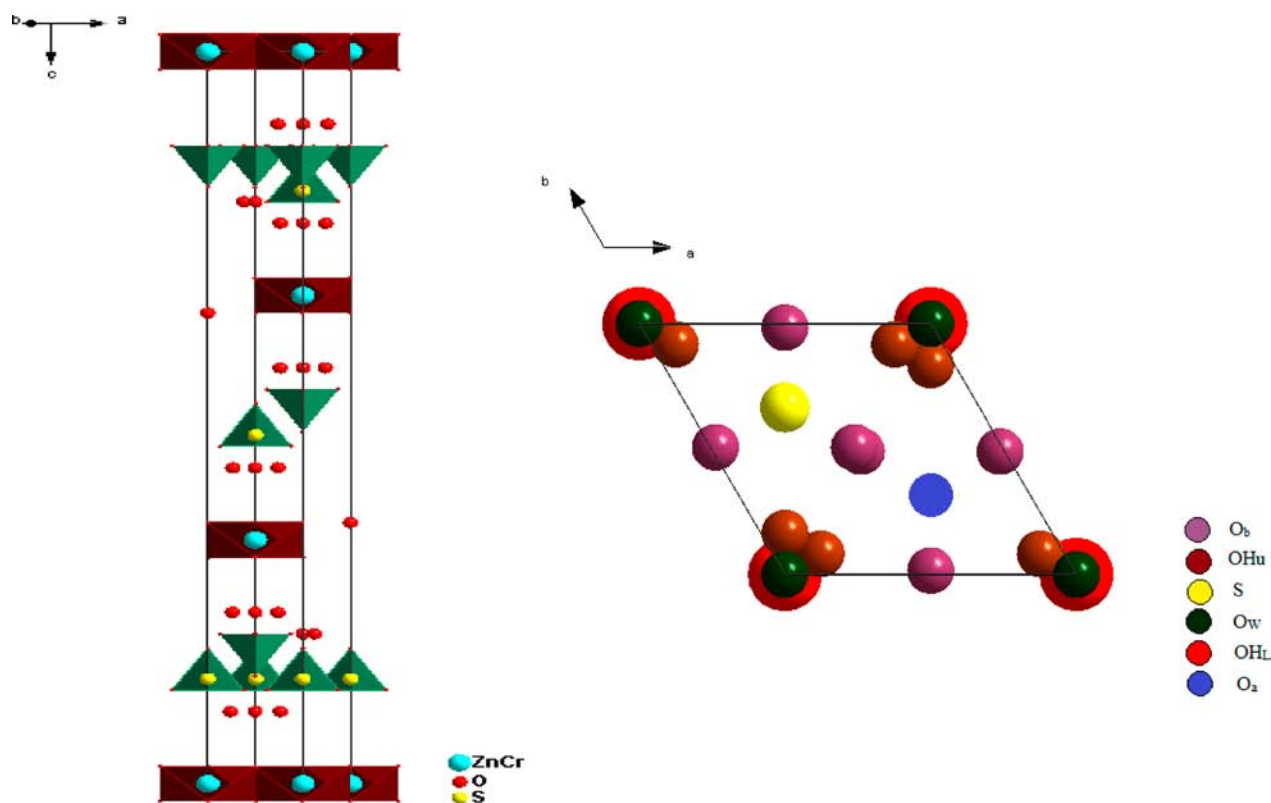


**Figure 6.** (a) Structure of [Zn–Cr]-HTPW-150 LDH viewed down the *y* direction, and (b) interlayer structure viewed down the *c* axis with the lower and upper hydroxyl O atoms of the adjacent layers.

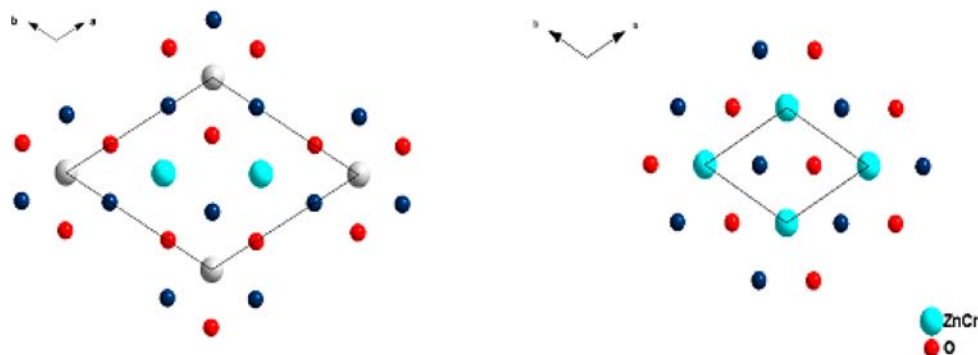


**Figure 7.** Structure of a single layer viewed down the  $c$  axis of (a) cation-ordered LDH and (b) cation-disordered LDH.

[Zn–Cr], [Cu–Cr], and [Mg–Fe], and it was shown that for all compositions there are no trivalent–trivalent near neighbors.<sup>34–36</sup> While the absence of such an interaction indicates cation ordering for 2:1 ( $x = 0.33$ ) LDHs over larger length scales, it does not indicate similar ordering for higher ratios ( $x < 0.33$ ). It was concluded that the ordering improves with an increase in trivalent metal content in the layer. However, evidence for long-range cation order by PXRD has not been reported among LDHs to date. The intensity of supercell reflections if any diminished drastically with even a slight deviation from perfect ordering.<sup>6</sup> There could be three reasons for this.

- (1) Supercell reflections arising out of cation order are intrinsically weak and therefore not observable.
- (2) Cation ordering cannot be detected by PXRD due to the similar scattering powers of the two metal ions in most LDH systems
- (3) The composition of the LDHs generally departs from the nominal value  $x = 0.33$ .

Evidence for cation order in mineral LDHs with different metal ratios in the layer has been reported where single-crystal diffraction data are available, and the structures have also been determined.<sup>27,28,37</sup> If 2 were right, then cation ordering should have been more evident in the [Zn–Al] LDH. Cation ordering limits the number of possible polytypes to (i) only one two-layered polytype of hexagonal symmetry ( $2H$ ) and (ii) only one three-layered polytype of rhombohedral symmetry ( $3R$ ). This is in contrast to three possible two-layered polytypes of hexagonal symmetry ( $2H_{1-3}$ ) and two different three-layered polytypes of rhombohedral symmetry ( $3R_{1-2}$ ) predicted by Bookin and Drits<sup>17</sup> for cation-disordered LDHs. In the [Zn–Al] system, observation of a  $3R_2$  polytype distinct from  $3R_1$  provides strong evidence for the absence of cation ordering. The amphotericity of  $\text{Al}(\text{OH})_3$  and the relatively higher pH of formation of the [Zn–Al] LDH point to the possible partial dissolution of  $\text{Al}^{3+}$  during synthesis and workup.

[Zn–Cr] LDH is one of the systems that has been extensively examined using EXAFS and is reported to have cation-ordered structures irrespective of the anion in the interlayer.<sup>34</sup> The cation-ordered  $1H$  structure observed for the hydrothermally treated sample [Zn–Cr]-HT-125 provides the first ever direct evidence for long-range cation ordering by powder diffraction.

We then ask the question is the as-prepared [Zn–Cr] LDH cation ordered? The as-prepared [Zn–Cr] LDH exhibits a basal spacing of 8.9 Å. The presence if any of the weak supercell reflections overlaps with the 002 basal reflection and is not observed. Upon hydrothermal treatment of the precipitate in

the mother liquor, the interlayer gets hydrated to form a LDH with an extended basal spacing of 11 Å and supercell reflections appear, indicating cation ordering. When the same as-prepared LDH is hydrated under ambient conditions or hydrothermally treated in water, the resultant phase has the structure of the  $3R_1$  polytype with  $a = 3.12$  Å, indicating the absence of cation ordering. This indicates that the as-prepared LDH is perhaps not cation ordered.

Two possibilities can be envisaged during hydrothermal treatment in mother liquor: (i) the layer of the as-prepared LDH dissolves and reprecipitates with cation order during hydrothermal treatment, (ii) the appearance of supercell reflections on hydrothermal treatment in mother liquor is due to sulfate ordering in the interlayer. According to Drits and co-workers,<sup>1</sup> cation ordering in the layer and ordering in the interlayer are linked due to electrostatic interactions between  $\text{M}^{3+}$  and the anion. During hydrothermal treatment in water, the higher pH prevents dissolution–reprecipitation and we observe a greater degree of interslab ordering arising due to rigid translation of the layers in the case of [Zn–Cr]-HTPW-150.

Other interesting features observed in this work are formation of the rare  $3H$  and  $3R_2$  polytypes on hydrothermal treatment of the [Zn–Al] LDH prepared at pH 9.

## CONCLUSIONS

Hydrothermal treatment of the sulfate-intercalated LDHs of [Zn–Al] and [Zn–Cr] carried out under a variety of conditions resulted in several structural transformations. While within the [Zn–Al] system we observe two unusual polytypes, in the case of the [Zn–Cr] system there is cation ordering in the layer, which exhibits supercell reflections in the PXRD pattern.

## ASSOCIATED CONTENT

### Supporting Information

PXRD patterns of as-prepared and hydrothermally treated [Zn–Cr] LDHs, snapshots taken during the structure optimization of [Zn–Cr]-HT-125 using code FOX and POWDERCELL simulations of [Zn–Cr]-HT-125 LDH with and without interlayer sodium. This material is available free of charge via the Internet at <http://pubs.acs.org>.

## AUTHOR INFORMATION

### Corresponding Author

\*E-mail: [vishnukamath8@hotmail.com](mailto:vishnukamath8@hotmail.com).

### Notes

The authors declare no competing financial interest.

## ACKNOWLEDGMENTS

The authors thank the Department of Science and Technology (DST), Government of India (GOI), for financial support. S.R. thanks the Council for Scientific and Industrial Research, GOI, for the award of a Senior Research Fellowship. P.V.K. is a recipient of the Ramanna Fellowship of the DST.

## REFERENCES

- (1) Drits, V. A.; Bookin, A. S. Crystal Structure and X-ray Identification of Layered Double Hydroxides. In *Layered Double Hydroxides: Present and Future*; Rives, V., Ed.; Nova Science: New York, 2001; pp 39–92.
- (2) Bellotto, M.; Rebours, B.; Clause, O.; Lynch, J.; Bazin, D.; Elkaim, E. *J. Phys. Chem.* **1996**, *100*, 8527.
- (3) Radha, A. V.; Shivakumara, C.; Kamath, P. V. *Clays Clay Miner.* **2005**, *53*, 521.
- (4) Menetrier, M.; Han, K. S.; Demourgues, G. L.; Delmas, C. *Chem. Mater.* **1997**, *36*, 2441.
- (5) Martin, M. J. S.; Villa, M. V.; Camazano, M. S. *Clays Clay Miner.* **1999**, *47*, 777.
- (6) Evans, D. G.; Slade, R. C. T. Structural aspects of Layered Double Hydroxides. In *Layered Double Hydroxides*; Duan, X., Evans, D. G., Eds.; Springer: New York, 2005.
- (7) Nickel, E. H.; Clarke, R. M. *Am. Mineral.* **1976**, *61*, 366.
- (8) Cavani, F.; Trifiro, F.; Vaccari, A. *Catal. Today* **1991**, *11*, 173.
- (9) Crepaldi, E. L.; Pavan, P. C.; Valim, J. B. *J. Braz. Chem. Soc.* **2000**, *11*, 64.
- (10) Radha, A. V.; Kamath, P. V.; Shivakumara, C. *Acta Crystallogr., Sect. B* **2007**, *B63*, 243.
- (11) Kovanda, F.; Rojka, T.; Bezdicka, P.; Jiratova, K.; Obalova, L.; Pacultova, K.; Bastl, Z.; Grygar, T. *J. Solid State Chem.* **2009**, *182*, 27.
- (12) Rabenau, A. *Angew. Chem., Int. Ed. Engl.* **1985**, *24*, 1026.
- (13) Sharma, S. K.; Kushwaha, P. K.; Srivastava, V. K.; Bhatt, S. D.; Jasra, R. V. *Ind. Eng. Chem. Res.* **2007**, *46*, 4856.
- (14) Xu, Z. P.; Stevenson, G. S.; Lu, C. Q.; Lu, G. Q.; Bartlett, P. F.; Gray, P. P. *J. Am. Chem. Soc.* **2006**, *128*, 36.
- (15) Drits, V. A.; Sokolova, T. N.; Sokolova, G. V.; Cherkashin, V. I. *Clays Clay Miner.* **1987**, *35*, 401.
- (16) Lyi, N.; Fujii, K.; Okamoto, K.; Sasaki, T. *Appl. Clay Sci.* **2007**, *35*, 218.
- (17) Bookin, A. S.; Drits, V. A. *Clays Clay Miner.* **1993**, *41*, 558.
- (18) Radha, S.; Kamath, P. V. *Cryst. Growth Design* **2009**, *9*, 3197.
- (19) Radha, S.; Antonyraj, C. A.; Kamath, P. V.; Kannan, S. Z. *Anorg. Allg. Chem.* **2010**, *636*, 2658–2664.
- (20) Lasocha, W.; Lewiniski, K. *PROSZKI, A System of Programs for Powder Diffraction Data Analysis*, ver-2.4, 1994.
- (21) Larson, A. C.; Von Dreele, R. B. General Structure Analysis System (GSAS). *Los Alamos National Laboratory Report LAUR*, 2004; p 86.
- (22) Nicolin, V. F.; Cerny, R. *J. Appl. Crystallogr.* **2002**, *35*, 734.
- (23) Fox, *Free Objects for Crystallography*, <http://objcryst.sourceforge.net>.
- (24) Bookin, A. S.; Drits, V. A. *Clays Clay Miner.* **1993**, *41*, 551.
- (25) Radha, S.; Prasanna, S. V.; Kamath, P. V. *Cryst. Growth Design* **2011**, *11*, 2287.
- (26) Boehm, H. P.; Steinle, J.; Viewger, C. *Angew. Chem.* **1977**, *16*, 265.
- (27) Cooper, M. A.; Hawthorne, F. C. *Can. Mineral.* **1996**, *34*, 91.
- (28) Humnicki, D. M. C.; Hawthorne, F. C. *Can. Mineral.* **2003**, *41*, 79.
- (29) Christiansen, B. C.; Balic-Zunic, T.; Petit, P. O.; Frandsen, C.; Morup, S.; Geckeis, H.; Katerinopoulou, A.; Stipp, S. L. S. *Geochim. Cosmochim. Acta* **2009**, *73*, 3579.
- (30) Ennadi, A.; Khaldi, M.; De Roy, A.; Besse, J. P. *Mol. Cryst. Liq. Cryst. Sci. Technol. A* **1994**, *244*, 373.
- (31) Britto, S.; Kamath, P. V. *Inorg. Chem.* **2011**, *50*, 5619.
- (32) Sideris, P. J.; Nielson, U. G.; Gan, Z.; Grey, C. P. *Science* **2008**, *321*, 113.
- (33) Vucelic, M.; Jones, W.; Moggridge, G. D. *Clays Clay Miner.* **1997**, *45*, 803.
- (34) Roussel, H.; Briois, V.; Elkaim, E.; de Roy, A.; Besse, J. P. *J. Phys. Chem. B* **2000**, *104*, 5915.
- (35) Sideris, P. J.; Blanc, F.; Gan, Z.; Grey, C. P. *Chem. Mater.* **2012**, *24*, 2449.
- (36) Bigey, L.; Depege, C.; de Roy, A.; Besse, J. P. *J. Phys. IV Fr.* **1997**, *7*, 249.
- (37) Hofmeister, W.; Platen, H. V. *Crystallogr. Rev.* **1992**, *3*, 3.